Liquid Crystals
Publication details, including instructions for authors and subscription information:
http://www.informaworld.com/smpp/title~content=t713926090

Long alkyl chain dimethylammonioalkoxydicyanoethenolates as new zwitterionic thermotropic liquid crystals

A. Mathis; M. Galin; J. C. Galin; B. Heinrich; C. G. Bazuin

Online publication date: 06 August 2010

To cite this Article Mathis, A. , Galin, M. , Galin, J. C. , Heinrich, B. and Bazuin, C. G.(1999) 'Long alkyl chain dimethylammonioalkoxydicyanoethenolates as new zwitterionic thermotropic liquid crystals', Liquid Crystals, 26: 7, 973 — 984
To link to this Article: DOI: 10.1080/026782999204327
URL: http://dx.doi.org/10.1080/026782999204327

LIQUID CRYSTALS, 1999, VOL. 26, NO. 7, 973–984

Long alkyl chain dimethylammonioalkoxydicyanoethenolates as new zwitterionic thermotropic liquid crystals

A. MATHIS, M. GALIN, J. C. GALIN*
Institut Charles Sadron (CNRS-ULP), 6 Rue Boussingault,
67083 Strasbourg Cedex, France

B. HEINRICH
Institut de Physique et Chimie des Matériaux (CNRS-ULP), 23 Rue du Loess,
67037 Strasbourg Cedex, France

and C. G. BAZUIN
Centre de Recherche en Sciences et Ingénierie des Macromolécules (CERSIM),
Département de Chimie, Université, Laval, Cité Universitaire, Québec,
Canada G1K 7P4

(*Received 11 November 1998; in final form 28 January 1999; accepted 16 February 1999*)

The liquid crystalline thermotropic behaviour of a series of long alkyl chain dimethylammonioalkoxydicyanoethenolates of the type CH_3–$(CH_2)_{n-1}$–$N^+(CH_3)_2$–$(CH_2)_p$–O–CO–$C^-(CN)_2$ ($n = 10$–18, even values only, with $p = 2$, 3; $p = 4$ for $n = 16$) was analysed through differential scanning calorimetry, X-ray diffraction and polarizing optical microscopy. Smectic A, columnar and cubic mesophases were observed in addition to a crystalline phase. The crystalline structure corresponds to a single layered lamellar arrangement of molecules characterized by a tilt angle of the paraffin chains of about 50° and 56° for $p = 2$ and 3, respectively. Above the melting point (70–100°C), all amphiphiles *n-p*, except 10-2 and 12-3 which became immediately isotropic, display one or more mesophases: smectic A for 14-2, 16-2, 16-3, 18-2 and 18-3 (zwitterionic bilayers with a thickness of about 12 Å), a hexagonal columnar phase for 12-2, 14-3 and 16-4 (monotropic for 12-2, zwitterionic cylinders of radius of about 12 Å), and an inverted bicontinuous cubic phase (*Ia3d* space group) for 14-2, 16-3 and 18-3 (rod-like elements of radius of about 10 Å). For 14-2 and 18-3, the cubic mesophase tends to form slowly from the smectic A phases both on heating and cooling. The amphiphiles displaying the columnar mesophase possess the lowest and an identical ratio of alkyl tail length to zwitterion length. The temperature range of mesophase stability is a strongly increasing function of n and a decreasing function of p. For the longest alkyl tail, mesophases extend over more than 130°C up to the degradation temperatures ($T \geqslant 210$°C). Strong dipolar interactions between the zwitterionic groups in their stretched conformation ($\mu > 25$ D) within the liquid apolar and incompatible paraffin matrix are the driving force for the thermotropic behaviour of these new amphiphiles.

1. Introduction

In the course of current work on zwitterionic polymeric materials [1], we became familiar with zwitterionic structures of the quaternary ammonioalkoxydicyanoethenolate type (*a* in the scheme), synthesized for the first time forty years ago [2]. They display a number of very specific properties such as:

(1) A strong delocalization of the negative charge over a hydrophobic acylmalononitrile moiety, which results in high stability and water insolubility.
(2) An unusually high dipole moment arising from high intercharge distances: for example, $\mu = 25.9$ and 30.8 D for $p = 2$ and 3, respectively, as derived from dielectric measurements on trifluoroethanol solutions for the triethylammonio derivatives [3].

*Author for correspondence.

Journal of Liquid Crystals ISSN 0267-8292 print/ISSN 1366-5855 online
http://www.tandf.co.uk/JNLS/lct.htm
http://www.taylorandfrancis.com/JNLS/lct.htm

(3) A very strong dipolar aprotic character leading to total immiscibility with apolar or weakly polar solvents or microenvironments.

a

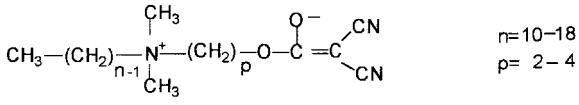

n=10–18
p= 2–4

b

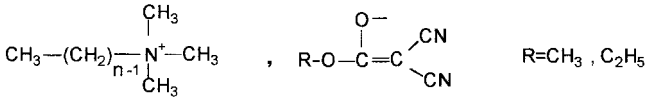

R=CH_3 , C_2H_5

We recently took advantage of this last feature for the design of segmented poly(tetramethyleneoxide) zwitterionomers: self-association of the dipolar functions unsolvated by the apolar matrix readily leads to their microphase separation and to the development of long range order in the bulk materials [4, 5]. In a simpler application, these zwitterions may be considered as attractive, if exotic, dipolar heads for new amphiphilic, low molecular mass species. With this in mind, long alkyl chain dimethylammonioalkoxydicyanoethenolates were recently synthesized and studied with respect to their self-association in dimethylsulfoxide as a selective polar solvent of the zwitterionic moieties [6].

The purpose of the present work is to analyse the potential thermotropic properties of these zwitterionic amphiphiles through X-ray scattering (WAXS and SAXS), polarizing optical microscopy (POM) and differential scanning calorimetry (DSC) as a function of the length of the alkyl tail [$n = 10$–18 (even values only) for $p = 2$ or 3] and of their intercharge spacer or tether length ($p = 2$–4 for $n = 16$), as shown in *a* in the scheme. In comparison with the much studied class of ionic, fully organic thermotropic systems of aliphatic quaternary ammonium or pyridinium salts [7–10], this homologous series of new amphiphilic compounds may be of special interest precisely because of the zwitterionic structure of the polar head groups. First, the directed dipolar interactions in these structures cannot be strictly identified with coulombic interactions (occurring, for instance, in the closely related ammonium salts given in *b* in the scheme), and some quantum chemical calculations on the packing mode of analogous zwitterions (ammonioalkylsulphonate type) have already been performed [11]. Moreover, the thermotropic behaviour of zwitterionic amphiphiles is much less documented than that of their lyotropic properties [12, 13] (see, in particular, the case of the natural phospholipids). *N*-alkyl-substituted iminodiacetic acids are a recent example of zwitterionic thermotropes where hydrogen bonding also plays a significant role [14]. Second, the possible thermal equilibrium between two zwitterion conformations [15], corresponding to a fully extended and a curled conformation ($\Delta\mu \sim 8.3$ and 14.6 D for $p = 2$ and 3, respectively [3]), may result in specific thermotropic behaviour related to this unique structural change.

Throughout the text, the successive figures, *n-p*, signify the number of carbon atoms in the alkyl tail and in the intercharge spacer (tether), respectively. Thus, amphiphile 16-3 possesses an alkyl tail of sixteen carbon atoms and a tether of three methylene groups within the zwitterionic moiety.

2. Experimental

2.1. *Materials*

The synthesis and purification by recrystallization of the compounds studied are already reported in the literature [6], except for sample 10-2 which was prepared according to the same general procedure.

Decyl derivative, 10-2, $C_{18}H_{31}O_2N_3$: Elemental analysis: calcd, C 67.25, H 9.72, O 9.95, N 13.07; found C 67.28, H 9.82, O 10.06, N 13.05%. ^{1}H NMR (DMSO) δ ppm: 0.85 (3H, CH_3); 1.24 (14H, CH_3–$(CH_2)_7$); 1.63 (2H, $CH_2CH_2CH_2N^+$); 3.03 (6H, $N^+(CH_3)_2$); 3.23 (2H, $CH_2CH_2CH_2N^+$); 3.52 (2H, $N^+CH_2CH_2O$); 4.30 (2H, CH_2O).

All the analytical data (^{1}H NMR and elemental analysis) reported in [6] indicate a high purity, like those for the decyl derivative given here. The samples were dried under reduced pressure at 60°C for 1–2 days, and stored either in airtight containers or in a dessicator containing silica gel.

2.2. *Physical measurements*

Thermogravimetric measurements were performed using a Mettler TA-3000 thermobalance under a constant nitrogen flow (flow rate of 200 ml min^{-1}) and at a heating rate of 2°C min^{-1}.

DSC measurements were performed mainly using a Perkin Elmer DSC-4 apparatus interfaced with a computer data station after previous calibration with indium for melting temperatures and enthalpies ($T_m = 156.6$°C, $\Delta H_m = 28.5$ J g^{-1}). About 5–10 mg of the previously recrystallized sample were weighed to an accuracy of ± 0.03 mg in aluminum pans which were immediately sealed. The same thermal cycle was systematically used for all samples: heating from 20 to 160°C at a heating rate of 1°C min^{-1} and cooling down to 0°C at a cooling rate of 5°C min^{-1}. When found necessary, other temperature limits were used to complete the initial data, in

some cases using a Perkin Elmer DSC-7 apparatus. The melting, crystallization and mesophase transition temperatures were determined at the maximum of the corresponding endothermic or exothermic peaks. They are reproducible unless otherwise noted to within ± 1°C, whether determined on freshly prepared samples or samples stored for a long time, and the accuracy on the melting ΔH_m values is better than ± 3%.

Complementary visual observations were made using a Zeiss Axioskop polarizing optical microscope (POM), equipped with a Leica objective, a Mettler FP52 hotplate and a Mettler FP5 controller. High temperature transitions were obtained using the POM only.

Wide and small angle X-ray scattering measurements were performed between 20 and 200°C using two experimental devices operating with linear collimation (infinite height slit conditions) of a monochromatic X-ray beam of $\lambda = 1.54$ Å (Cu K_α) on samples previously sealed in Lindemann glass capillaries. The scattered beams were recorded on photographic films (Guinier camera) for scattering vectors q in the range 0.06–2.5 $Å^{-1}$ in the first device and on an INEL CPS-120 curved position-sensitive detector in the second device. Measurements were made by stepwise heating of the sample up to a maximum of 200°C, followed by stepwise cooling to room temperature (5°C steps).

2.3. *X-ray data treatment*

The nature of the various mesophases was identified in the usual way from the ratios of the successive Bragg reflections. The corresponding geometrical parameters of the zwitterionic domains were derived from the dimension of the elementary cell, the volume V_z and the volume fraction Φ_z of the zwitterionic moiety in the amphiphile according to classical space filling calculations. They are detailed in the literature for the more complex case of the cubic lattice of the *Ia3d* space group [16, 17].

The volume fractions of paraffin and of the zwitterionic moiety [Φ_z, related to $N^+(CH_3)_2$–$(CH_2)_p$–O–CO–C–$(CN)_2$] in the amphiphiles were derived, to a first approximation, from their corresponding weight fractions and densities, assuming a simple additivity rule for the calculation of the specific and molar volumes (V_m). The densities were taken to be identical to that of the paraffin of the same chain length, n, and to that of model triethylammonio zwitterions [3] (v/ml g^{-1} at 25°C = 0.756 for $p = 2$ and 0.762 for $p = 3$), respectively. Taking into account the previous approximations and assuming an average thermal volume expansion of 5% for a representative temperature increase of 100°C, the accuracy on the Φ_z is about ± 5% and the molar volume V_m in the liquid crystalline phases is probably underestimated on average by about 5%.

3. Results and discussion

According to thermogravimetric analysis of representative samples under a nitrogen atmosphere, the initial degradation temperatures, as conventionally measured at 5% weight loss, are 213 and 225°C for samples 16-2 and 16-3, respectively, as compared to 220°C for triethylammonioethoxydicyanoethenolate chosen as a model zwitterion. The maximum temperature for the physical measurements was thus fixed at 200°C (unless otherwise specified).

The mesogenic characteristics of the entire series of zwitterionic compounds studied, as determined by the various methods used and as will be detailed subsequently, are summarized in table 1. It can be observed that all samples except 10-2 and 12-3 possess one or more disordered mesophases in addition to the crystalline phase. These mesophases have been identified as hexagonal columnar, inverted bicontinuous cubic and smectic A.

3.1. *Crystalline phases*

3.1.1. *DSC measurements*

For all samples, the thermograms recorded on heating show a strong endothermic peak (width about 4–5°C) in the temperature range 50–100°C, related to the crystal–isotropic (Cr-I) or crystal–mesophase (Cr-M) transition. Recrystallization systematically occurs at a much lower temperature than melting and, in fact, the corresponding exotherms, of strongly reduced intensity, are observed at $T > 0$°C only for the species with longer alkyl tails, 16-2, 18-2 and 18-3. The fraction of crystallized material obtained after melting, in the cooling conditions used, is lower than 40% (neglecting the temperature dependence of the melting enthalpy). Zwitterions bearing the shorter alkyl tails remain in the supercooled state at room temperature for several days before recrystallization occurs. These kinetic effects, and especially the supercooling of often more than 80°C, are unusually strong. They may be ascribed to the much increased viscosity of the non-crystallized milieu resulting from the strong dipolar interactions between the zwitterionic heads.

In some cases, it was noted that the melting peak is sensitive to sample and thermal history, as well as to scan speeds (multiple peaks sometimes appear at faster scans), although this was not systematically studied. This was particularly evident for sample 12-2. This generally shows either a single high enthalpy peak near 75°C, when recrystallized from solution, or a predominant peak at 67°C usually accompanied by a transition at 75°C of much lower intensity when recrystallized from the melt, as if two crystalline forms are involved (as indicated also by POM observations). This particular behaviour was not generally observed in the other samples ($n > 12$) and the study of a potential crystalline

Table 1. Thermal data for the *n-p* amphiphiles (peak transition temperatures, T (°C), and enthalpies, ΔH (kJ mol^{-1}); values in parentheses are the data obtained on cooling).

Compound	Cr	$T/\Delta H$	Col_h	$T/\Delta H$	Cub	$T/\Delta H$	SmA	$T/\Delta H$	I
10-2	•	53/27							•
	•	(-)							•
12-2	•	75/37[a]	•[b]	68/0.3[b]					•
	•	(-)	•	(64/ – 0.3)					•
12-3	•	87/26							•
	•	(-)							•
14-2	•	78/45[c]			•	114/0.4	•[c]		•
	•	(-)			•	(-)[c]	•	(110/ – 0.3)	•
14-3	•	93/33	•	107/0.4					•
	•	(-)	•	(104/ – 0.3)					•
16-2	•	84/54					•	199[d]	•
	•	(9/ – 8)					•	([f])	•
16-3	•	95/39			•	156/0.2	•	159/0.2	•
	•	(-)			•	(109/ – 0.1)	•	(157/ – 0.2)	•
16-4	•	93/35	•	96/0.2					•
	•	(-)	•	(92/ – 0.2)					•
18-2	•	89/63					•	~245[d]	•
	•	(38/ – 22)					•	([f])	•
18-3	•	97/52[c]			•[c]	117/0.3[c]	•	~230[d]	•
	•	(27/ – 20)			•[c]	(-)	•	([f])	•

[a] Data for a crystallized sample (another crystal form appears at 67°C; see text for details).
[b] Data for a non-crystallized sample; monotropic phase.
[c] Slow kinetics for cubic phase development, unmasking SmA phases (see text for details).
[d] Data obtained from polarizing optical microscopy.
[f] Not given, since affected by degradation.

polymorphism in these zwitterionic amphiphiles was beyond the scope of the present work.

For $n \geqslant 12$ (considering the higher temperature peak for sample 12-2), the melting temperature $T_{Cr\text{-}M/I}$ is an increasing, quasi-linear function of the alkyl tail length (1.8 and 2.4°C/CH_2 for $p = 2$ and 3, respectively), with $T_{Cr\text{-}M/I}$ ($p = 3$) being systematically higher than $T_{Cr\text{-}M/I}$ ($p = 2$) by 9–15°C. This last feature contrasts with the reverse order found for the melting temperatures of the corresponding triethylammonio zwitterions: $T_m = 187$ and 148°C for $p = 2$ and 3, respectively [3]. The significant decrease in T_m observed when going from these model compounds (compare also with $T_m = 212$°C for trimethylammonioethoxydicyanoethenolate [2]) to the thermotropic species and the T_m increase with alkyl tail length are analogous to those already noted for copper (II) soaps [18], for instance. This common behaviour shows that the thermal stability of the crystal is finely tuned by two contributions: the strong dipolar interactions among the zwitterions and the ordering of the paraffin chains, their respective weights reflecting the chemical structure of the species. The lower T_m value observed for the shortest alkyl tail, sample 10-2, may tentatively be correlated with a strong decrease in the thermal stability of the crystals, whose structure and cohesion may be mainly determined by the zwitterionic polar head groups, but strongly perturbed by the rather short alkyl chains. Conversely, increased ordering of the longer paraffinic tails enhances the thermal stability of the crystals. Possibly, the apparent sensitivity of the melting behaviour of amphiphile 12-2 to sample history (sometimes having a lower T_m like sample 10-2, sometimes having a T_m consistent with the linear behaviour of the other amphiphiles) reflects its borderline position between sample 10-2 and those with longer alkyl tails.

The Cr–M/I transition enthalpies are also an increasing linear function of the alkyl tail length, as illustrated by the following good correlations [$R(x)$ = regression coefficient on x data points):

$$p = 2, n \geqslant 10,$$
$$\Delta H/\text{kJ mol}^{-1} = 4.425n - 16.5, \quad R(5) = 0.9997;$$
$$p = 3, n \geqslant 12,$$
$$\Delta H/\text{kJ mol}^{-1} = 3.445n - 15.6, \quad R(4) = 0.9847.$$

The slopes directly measure the melting enthalpies per methylene group of the alkyl tail, giving values of 316 and 303 J g^{-1} for $p = 2$ and 3, respectively. This is in good agreement with the classical value of 289 J g^{-1} typical of linear paraffins (difference less than 10%) [19], although a little higher than the value of 272 J g^{-1} often found for the melting of paraffin chains in smectic mesogens [20].

3.1.2. *X-ray scattering measurements*

For all the amphiphiles, the X-ray diffraction patterns of the crystal phase (solution-crystallized samples) show a number of Bragg reflections, at both small and wide angles, which correspond to a three dimensional lamellar packing of the molecules. Only the variations of the lamellar spacings d ($d \pm 0.5$ Å, first Bragg reflection in the SAXS pattern) with the length n of the paraffin tail will be discussed successively for the two homologous series, $p = 2$ and 3 (see table 2).

For the amphiphile series n-2, the experimental data lead to the correlation:

$$d/\text{Å} = 7.45 + 0.815n, \quad R(5) = 0.9940.$$

The length increment per methylene group of 0.82 Å is significantly lower than that expected for an all-*trans*-paraffin chain of 1.27 Å. On the other hand, the intercept of 7.4 Å is in good agreement with the intercharge distance of 6.0 Å calculated for the dipolar head of triethylammonioethoxydicyanoethenolate in its fully stretched conformation [3], noting that the calculated distance is that between the centres of gravity of the two charges and is therefore a little shorter than the overall length.

The lamellar structure thus very probably corresponds to a single layered arrangement of molecules characterized by a tilt angle of the paraffin tails of about 50°, most likely with the molecules pointing alternately in opposite directions, as shown in figure 1. Although the experimental data do not permit analysis of the internal structure of the zwitterionic layer, the proposed arrangement is consistent with an antiparallel alignment of the dipoles in their extended conformation, which is, in fact, the preferred packing mode according to molecular mechanics and quantum chemical calculations performed for similar zwitterions of the n-hexyldimethylammonioalkylsulphonate type $[C_6H_{13}–N^+(CH_3)_2–(CH_2)_p–SO_3^-]$, $p = 1, 3, 4$ [11].

Knowledge of the molar volume V_m and of the lamellar spacing d allows us to estimate directly the surface area per molecule available at the interface, $S = V_m/d$,

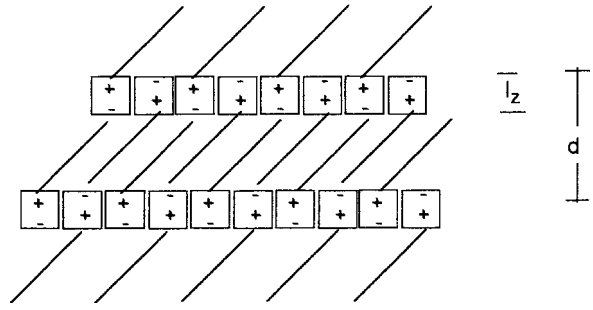

Figure 1. Schematic view of the single layered arrangement of the n-p amphiphiles in the crystalline state.

Table 2. Typical Bragg distances, d, observed in the X-ray patterns and thermal expansion coefficients of the structural parameter d_1 for the various n-p amphiphiles.

Compound	d (cryst)[a]/Å	T[b]/°C	d_n (mesophase)[c]/Å				d (WAXS)[d]/Å	Structure	$1/d_1\,[\delta d_1/dT]$ /°C^{-1} × 10^{-4}
			d_1	d_2	d_3	d_4			
10-2	15.5	70	26.0[e]					I	
12-2	17.5	65[f]	30.7	17.8	15.5		4.7	Col_h	– 9.7
12-3	17.0	100	27.5[e]					I	
14-2	18.5	104	32.0	15.8			4.9	SmA	
		109	32.8	28.3	19.6		4.9	Cub	– 8.2
		150	31.0[e]					I	
14-3	18.8	95	33.3	19.6	16.4		4.7	Col_h	– 8.0
		120	29.8[e]					I	
16-2	10.8	90	33.6	16.8			4.7	SmA	– 8.0
		140	33.1	16.6			4.7	SmA	– 8.0
16-3	20.0	100	35.2	30.4	22.4	18.5	4.8	Cub	– 7.5
		162	35.8[e]					I	
16-4	19.2	95	33.6	19.3			4.6	Col_h	
18-2	22.1	90	36.3	18.1			4.6	SmA	– 7.4
		150	34.2	17.3			4.6	SmA	– 7.4
18-3	21.3	100	38.5	33.3			4.6	Cub	– 6.8
		120	35.4	17.8			4.6	SmA	– 6.6

[a] First order reflection of the crystalline phase, measured at 25°C.
[b] Temperature of measurement for the mesophase.
[c] Subscript n in d_n indicates the order of the reflection involved.
[d] Determined from the maximum of the wide angle halo in the mesophase.
[e] Diffuse band.

$S \sim 36$ Å^2 with an accuracy of about 8%. This rather high value reflects, on the one hand, the significant tilt angle of the alkyl chains. On the other hand, combined with the conclusion from the intercept value that the zwitterion moities are oriented normal to the lamellar plane, the value of S implies that the zwitterions are almost as thick (6 Å) as they are long.

For the amphiphile series n-3, the experimental data lead to the correlation:

$$d/\text{Å} = 8.62 + 0.711n, \quad R(4) = 0.9969.$$

As in the previous case, the data for this series are consistent with the same model of a single layered arrangement of molecules in a lamellar structure with tilted alkyl chains. The intercept of 8.6 Å is in good agreement with the intercharge distance of 7.3 Å for the zwitterionic moiety in its extended conformation [3]. The length increment per methylene group of 0.71 Å leads to a tilt angle of the paraffin chains of about 56°, corresponding to a surface area per molecule of 38 Å^2 available at the interface. It can be concluded that the three dimensional lamellar packing of the molecules appears to be similar for the two homologous series of amphiphiles.

3.2. *Liquid crystalline phases*

3.2.1. *Overview and thermal stability of the liquid crystalline phases*

As indicated in table 1, the majority of the zwitterionic amphiphiles studied show one or more additional transitions at temperatures above the melting peak. In all cases, these transitions are narrow (± 1°C) and of low enthalpy, consistent with transitions between disordered or liquid phases. The precise nature of these phases was identified by POM and X-ray diffraction.

For temperatures higher than the melting point of the alkyl tails and below the isotropic phase, the X-ray patterns of the amphiphiles generally show a well defined series of reflections at small angles (the peaks are sharper for the higher n values and, for a given sample, their relative intensities decrease with their order), the first order reflection corresponding to Bragg distances in the range of 25–40 Å, and a broad and diffuse band at wide angles whose maximum corresponds to a Bragg distance of 4.6–4.9 Å. Moreover, the small angle Bragg distances decrease approximately linearly with increasing temperature, and the longer the paraffin tails the weaker these variations are whatever the structure of the liquid crystalline phase. An overview of these X-ray data is given in table 2. All the features noted are consistent with liquid crystalline phases involving a liquid conformation of the paraffin tails, with coherence domains extending over longer distances for the higher n values.

The isotropic state is characterized by the persistence of a diffuse small angle peak typical of cybotactic structures [21, 22], by the lack of any anisotropy in POM observations, and by a significant increase in sample fluidity. It should be mentioned that the fluidity in the isotropic state is temperature dependent; in particular, non-crystallized isotropic samples such as 10-2 and 12-2 become very viscous as they are cooled to ambient temperature, as a result of strong dipolar interactions; this feature probably accounts for the very slow crystallization noted above.

In the POM, the smectic A phase could be readily identified by the formation of the homeotropic and the focal conic textures typical of this phase, such as is shown on the birefringent side of figure 2 (obtained during a heating scan, and therefore less well defined). Generally, the focal conics are relatively small in size and tend to be dispersed within a homeotropic matrix, especially after cooling from the isotropic phase. The columnar phase is characterized by the texture shown in figure 3 (obtained on cooling from the isotropic phase), with rather smooth and well defined focal conics, generally with four apexes meeting together. The cubic phase was unequivocally identified by the formation of a completely non-birefringent (black) texture accompanied by very high viscosity. In non-polarized light, the sample appears wrinkled in this phase.

Ignoring the type of mesophase concerned, it is observed that their thermal stability depends strongly on the alkyl tail and tether lengths. First, as is most evident when taking $p = 2$ and 3 separately, the temperature range of mesophase stability increases rapidly with increase in alkyl tail length. Thus, no mesophases are observed for 10-2 and 12-3, and only a monotropic mesophase for 12-2 (becoming isotropic, in the absence of crystallization, at a mere 68°C), whereas for the amphiphiles with the longest tails, 18-2 and 18-3, a mesophase exists at least up to degradation temperatures (well above 200°C). (It should be noted that, despite the degradation which occurs both before and simultaneously with the transition, the disordered mesophase reappears upon cooling.) This dramatic increase in mesophase stability with increasing alkyl tail length has been observed previously for thermotropic liquid crystals with ionic head groups [8].

Second, an increase in tether length has a destabilizing effect on the mesophase stability, as shown by fact that the thermal stability of the mesophases for $p = 3$ is systematically lower than that for $p = 2$. Thus, a monotropic mesophase is observed for 12-2 whereas none is observed for 12-3 despite the same suppression of recrystallization in both samples. The effect is particularly striking for the $n = 16$ series: the isotropization temperature is attained at a low 96°C for $p = 4$ (only a few

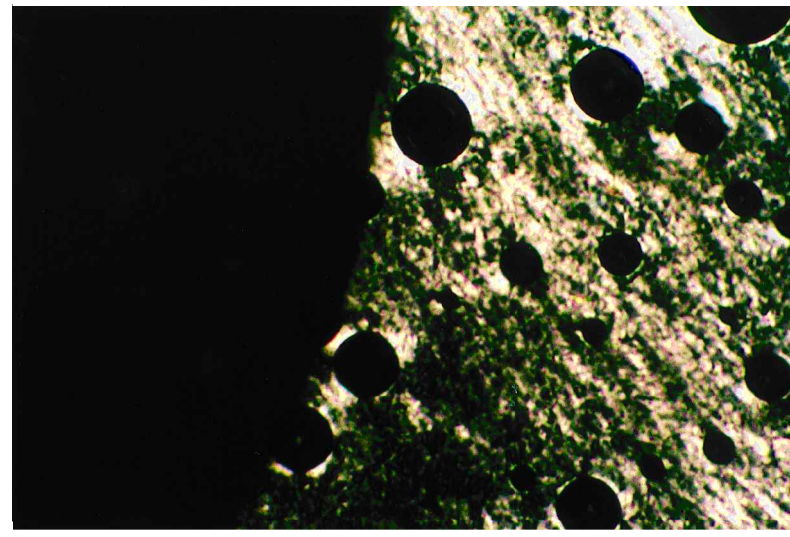

Figure 2. Polarizing optical micrograph taken during the progression of the cubic phase (black texture) into the smectic A phase (birefringent texture) in amphiphile 14-2 (taken at 85°C after heating from the crystalline state). The black circles are air pockets.

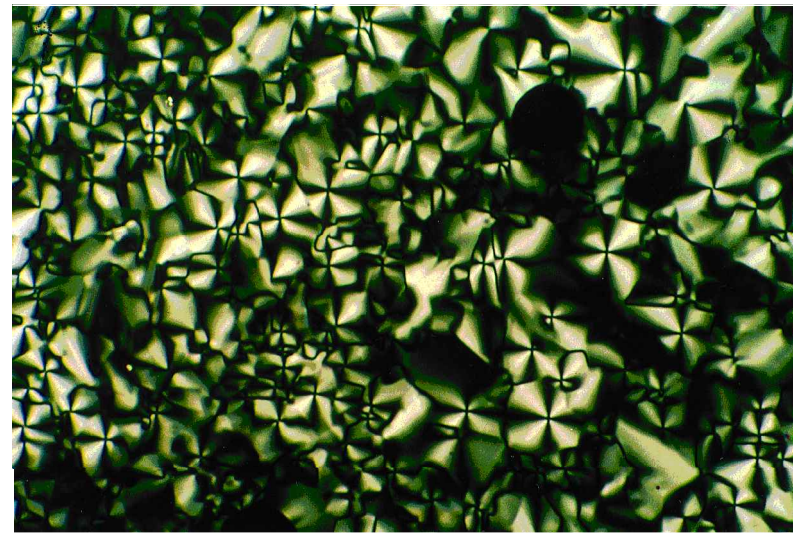

Figure 3. Polarizing optical micrograph of the columnar phase of amphiphile 12-2 (taken at 62°C after cooling from the isotropic state).

degrees above the melting peak), at 159°C for $p = 3$, and at 200°C for $p = 2$.

According to molecular mechanics calculations, dimerization through dipolar interactions is energetically more favoured when increasing the tether length from $p = 3$ to $p = 4$ in the homologous series of *N*-hexyl-*N*,*N*-dimethylammonioalkylsulphonates [11]. The behaviour observed for the amphiphile 16-4 is not consistent with this trend. However, because of significant differences in the geometry and polarizability of the anionic sites, it is not certain that the self-association thermodynamics of the two types of zwitterionic structures are parallel. Moreover, possible enhanced compatibility of the four methylene tether with the paraffinic chains may be less favourable to the development of sharp interfaces between the dipolar head and the alkyl chain.

The above trends are a reflection of the fact that the amphiphilic character of the molecules, which is the driving force for mesophase development, is an increasing function of the paraffin tail length and a decreasing function of the tether length in the zwitterionic head. Thus, the combined contributions of a low n and a high p explain the lack of any liquid crystalline phase in sample 12-3. This general behaviour may be compared with the lyotropic properties of a series of long alkyl chain zwitterionic amphiphiles of the dimethylammonioalkylethoxyphosphonate type: well organized lamellar mesophases are generally observed in concentrated aqueous solution, except for the shorter paraffin chain, $n = 12$, and the longer intercharge spacer, $p = 6$ [23].

It is of interest to note that a columnar phase appears only for samples 12-2, 14-3 and 16-4. A possibly significant correlation can be found by taking the experimental values (as determined in §3.1.2 from the intercepts of the Bragg distances of the crystalline phase as a function of alkyl tail length) for the length of the zwitterionic

segment for $n = 2$ and 3 (7.4 and 8.6 Å, respectively) and assuming that the analogous value for $n = 4$ can be obtained by adding the difference in values between $n = 2$ and 3 to the value for $n = 3$. Then, the length of the alkyl chain is almost exactly double (2.06 ± 0.02) that of the zwitterion segment for each sample possessing a columnar phase. We note this surprisingly consistent, if not coincidental correlation, but have no clear explanation to offer for it.

It is further noteworthy that no other liquid mesophase appears in the samples possessing the columnar phase. On the other hand, the smectic A and the cubic phases are frequently present in the same samples, noting also that, in all these cases, the alkyl chain length is more than twice the length of the zwitterionic segment†. Again, we have no specific explanation to offer, but suggest that the appearance of the disordered phases may depend on the respective proportions of alkyl chain and zwitterionic moiety in an analogous way to that observed for block copolymers, where it is well known that, depending on the relative proportion of the blocks involved, lamellar, columnar, cubic and bicontinuous cubic phases may be present [24].

POM observations indicate that the development of the cubic mesophase is characterized by relatively slow kinetics (as is frequently observed for this mesophase), which apparently depends on the amphiphile. For sample 14-2, the crystalline phase first melts into a smectic A phase, and on further heating, the cubic phase develops more or less slowly. This was clearly observed microscopically in that, after melting, a white birefringent texture which can be easily sheared first appears, and this is eventually overtaken by a black front which inexorably progresses across the field of vision; after this the sample is highly viscous. This progression at a particular instant in time is shown in figure 2. Thus, the sample was observed to transform *on heating* from a *less* viscous phase to a significantly *more* viscous phase. On further heating, the cubic phase melts directly to the isotropic phase (at 113.8°C), visible in the microscope by a dramatic decrease in viscosity (flowing of the sample). On cooling sample 14-2 from the isotropic phase, the SmA phase first appears (at 110.0°C) and then the cubic phase. The transition from the SmA phase to the cubic phase on either heating or cooling was not detected in the DSC thermograms; this may be related to the slowness of the transition. It should be noted that the smectic A phase obtained on heating and that obtained on cooling are not necessarily identical, but this was not further investigated.

The same phenomenon was observed by microscopy for amphiphile 18-3, although the cubic phase seems to develop with much more difficulty than for sample 14-2, and it was thus quite easy to miss in scanning the temperature range of interest. When it does appear, it transforms back to the smectic A phase (on heating) at 117°C (as detected by both DSC and microscopy). Furthermore, POM observations indicated that it was quasi-impossible to obtain a complete transformation to the cubic phase in this sample. In other words, the cubic and smectic A mesophases (and therefore fluid and highly viscous regions) were observed to *coexist*. Again, the transformation *from* the SmA phase *to* the cubic phase, on either heating or cooling, was not detected in the DSC thermograms.

Interestingly, in contrast to samples 14-2 and 18-3, the cubic phase in sample 16-3 is obtained directly from the crystalline phase, and then, at a higher temperature, transforms into a SmA phase which has a range of only 3°C before becoming isotropic. In this case, the transition from the SmA phase to the cubic phase on cooling *is* detected by DSC, and table 1 shows that it undergoes significant supercooling (almost 50°C).

Thus, it appears that the kinetics of the cubic phase development in the zwitterionic amphiphiles depend, at least in part, on the alkyl tail length (or its relative proportion). It should be added that it is also possible that minute amounts of bound H_2O, which may be difficult to remove (or difficult to prevent readsorption thereof during sample preparation and during experiments conducted in the ambient atmosphere, as is the case for polarizing optical microscopy), given the ionic nature of the amphiphile, may affect the kinetics [25]. These phenomena deserve detailed analysis in a future study.

3.2.2. *Structure of the liquid crystalline phases*

The geometrical parameters of the various phases and the corresponding aggregation numbers of the zwitterions (see §2) are given in table 3.

3.2.2.1. *Smectic A mesophase.* The X-ray data for the disordered lamellar structures obtained for amphiphiles 14-2, 16-2, 18-2 and 18-3 (reciprocal spacings in the ratio 1 : 2) indicate that the periodicity is strongly increased, by about 65%, compared with that observed in the crystal phase; this is much higher than would be expected from the usual thermal expansion when heating from 25 to 95–150°C (about 5%) and with the melting of

† The ratios of alkyl tail length to zwitterion length (calculated as described in the text) are: 2.39, 2.36 and 2.65 for 14-2, 16-3 and 18-3 (the amphiphiles which possess a cubic mesophase), respectively, and 2.73 and 3.07 for 16-2 and 18-2 (amphiphiles which possess a smectic A mesophase only), respectively. If significant, this suggests that, in this series of amphiphiles, the cubic phase develops for ratios of alkyl tail to zwitterion lengths intermediate to that required for the columnar phase and the higher ratios possible for smectic A development.

Table 3. Geometrical parameters and aggregation numbers determined for the mesophases of the various *n-p* amphiphiles (see text for definition of the symbols).

Mesophase	Compound	V_m (cm^3 mol^{-1})							
SmA			d_z/Å	S/Å^2					
	14-2	406	11.4	42.3					
	16-2	439	11.4	43.4					
	18-2	475	11.4	43.4					
	18-3	489	11.8	45.9					
Col_h			a/Å	Σ/Å$^2 \times 10^{-2}$	R_z/Å	S/Å^2	n_z	N_z	
	12-2	370	35.4	10.85	11.8	41.9	1.8	11.5	
	14-3	421	38.4	12.77	12.5	43.1	1.8	12.0	
	16-4	465	39.5	13.51	12.7	45.7	1.7	11.8	
Cub(*Ia*3*d*)			a/Å	V/Å$^3 \times 10^{-5}$	R_z/Å	b/Å	S/Å^2	n_z	N_z	N_c
	14-2	406	80.3	5.17	9.4	28.4	47.5	1.1	7.7	770
	16-3	453	86.2	6.40	10.0	30.5	48.9	1.2	9.1	850
	18-3	489	94.3	8.42	10.5	33.3	46.6	1.3	8.8	1030

materials (about 10%). In fact, d is now greater than a single molecular length, indicating that the phase is no longer single-layered, but either bilayered or partially bilayered. Furthermore, the tendency to form the homeotropic texture in this phase, as observed microscopically, argues that this is an orthogonal, and therefore a smectic A, phase. A possible arrangement is shown schematically in figure 4, with the zwitterionic moieties arranged in bilayers that alternate with a disordered alkyl sublayer of chains from facing zwitterionic layers.

Analysis of the surface area calculated for two molecules, S ($=2V_m/d$), is consistent with the structure of figure 4. Specifically, S is 42–46 Å^2 (table 3); this is much smaller than the equivalent surface area determined for the monolayer crystalline phase (72 Å^2 for two molecules), implying that the zwitterionic moieties must now be in a bilayer or partial bilayer arrangement. In the alkyl sublayer, given that S is about twice the transverse area of a single fully extended and melted alkyl chain [26], the chains from opposite zwitterionic layers may either not interpenetrate at all (in which case they are very disordered as shown in figure 4), or they may be completely interdigitated and stretched along the director. The amphipatic properties of the two molecular moieties would favour the latter alternative, although recent studies [27] suggest that interpenetration of alkyl chains occurs only when S is greater than 45 Å^2 near 100°C.

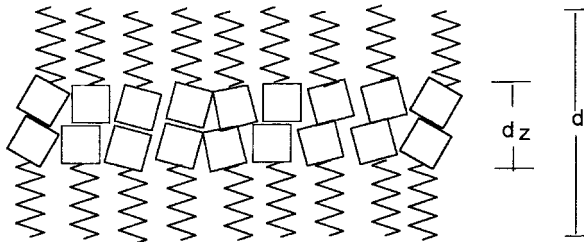

Figure 4. Schematic view of the double layered structure of amphiphiles 14-2, 16-2, 18-2 and 18-3 in their smectic A state.

The thickness of the zwitterionic bilayer, d_z, can be calculated from $d\Phi_z$ where Φ_z is the volume fraction of the zwitterion moiety (see §2). It is noteworthy that half of this value is significantly smaller than the length of the zwitterion moiety in its extended conformation for both $p=2$ and 3 (5.7 vs. 7.4 Å and 5.9 vs. 8.6 Å, respectively, as determined experimentally in §3.1.2). This can be explained by partial overlap of the two zwitterionic layers (partial bilayers), by an order parameter in this sublayer that is less than unity because of random tilting or bending of the zwitterionic moieties (favoured perhaps by the flexible tether), or even by the zwitterion moieties lying in the plane of the lamellae (recalling, in particular, the lateral thickness of 6 Å for the zwitterion moiety as suggested by the value of S in the crystalline phase). The present data do not, in fact, allow us to determine the exact disposition of the zwitterionic moieties relative to one another that optimizes dipolar interactions. However, it is worth mentioning that the zwitterions in an amorphous glassy zwitterionic polysoap such as poly{3-[*N*-(11-methacryloyloxyundecyl)-*N*,*N*-dimethyl] ammoniopropylsulphonate}, which is also organized in a lamellar structure, do not adopt a strictly antiparallel conformation and may be partially interdigitated with paraffin chains [28].

Finally, it must be added that, as is usual in smectic A phases [29], the lamellar spacing, d, decreases with increasing temperature, following the order parameter

decrease due to increasing thermal energy. Thus, the corresponding contribution to the dependence of S upon temperature has the same sign and a similar magnitude to that resulting from the volume expansion [20].

3.2.2.2. *Hexagonal columnar mesophase*. The structure identified for amphiphiles 12-2, 14-3 and 16-4 (reciprocal spacings in the ratio $1:\sqrt{3}:\sqrt{4}$) involves a two dimensional hexagonal lattice of cylinders corresponding to close packing of columnar zwitterionic aggregates surrounded by paraffin shells. Table 3 gives the distance a between the column axes, the lattice area Σ, the radius R_z of the columnar core (assumed to exhibit a circular section although this is far from certain), the molecular area S at the interface between the columnar core and the aliphatic crown and the number n_z of zwitterions involved in a columnar unit of height 1 Å. At the interface, the distance between neighbouring molecules should be the same along and around the columns, which is therefore close to $S^{0.5}$. The number of molecules needed to fill the columnar cross section is thus given by the number N_z of zwitterions involved in a columnar unit of height $S^{0.5}$ Å‡. The variations of the above geometrical parameters with n and p are very weak (table 3). However, the slight trend towards higher R_z and S values for higher p values is consistent with the corresponding increase in zwitterion size. All these structural features are highly reminiscent of those observed for rubbery semi-telechelic zwitterionic poly(isoprenes) of low molecular mass ($M_n < 5000$), bearing one dimethylammoniopropanesulphonate end group ($N^+(CH_3)_2$–$(CH_2)_3$–SO_3^-), which has the same hexagonal packing of zwitterionic cylinders of radius 13 Å [30].

It should be pointed out that d and therefore a, Σ, R_z, n_z, and N_z *decrease* with increasing temperature (see table 2). On the other hand, thermal expansion implies that, at least locally, S *increases* with increasing temperature as observed for the smectic A phase. This apparent contradiction, previously noted for other thermotropic series showing columnar and cubic mesomorphism [31], was explained by the fact that the columnar cores undulate. The variation of the packing parameters due to the thermal expansion therefore becomes hidden by the opposite variation due to increasing undulation.

3.2.2.3. *Cubic mesophase*. The X-ray data for the cubic mesophase identified for amphiphiles 14-2, 16-3 and 18-3 (reciprocal spacings in the ratio $\sqrt{6}:\sqrt{8}:\sqrt{14}:\sqrt{22}$) are specific for an inverted bicontinuous cubic lattice belonging to the $Ia3d$ space group. The structure consists of zwitterionic rod-like elements, all identical, joined three-by-three to form two three dimensional networks mutually interwoven and unconnected. A general picture of such a structure is given in refs. [13] and [16]. All the pertinent geometrical parameters are given in table 3: the lattice parameter a, the unit cell volume V ($=a^3$), the radius R_z of the zwitterionic rods, the rod length b (distance between two successive trifunctional junction points), the S, n_z and N_z values previously defined (see hexagonal mesophase), and the number N_c ($=V/V_m$) of molecules per lattice.

Analogous cubic phases are already classical for a number of ionic or zwitterionic surfactants in well defined conditions of temperature for pure materials or of concentration for hydrated systems [13, 16]. By comparison, semi-telechelic zwitterionic poly(isoprenes) of high molecular mass (zwitterionic volume fraction $\Phi_z \leqslant 0.01$) display liquid crystalline long range order corresponding to a body-centred cubic lattice characterized by zwitterionic microdomains of radius $R_z = 13$ Å, and of aggregation number, $N = 75$–110, depending on the poly(isoprene) chain length in the range $M_n \sim 14000$–28000 [30].

Despite thermal expansion, d_z, R_z, b, S and N_c decrease with increasing temperature: this behaviour is in good agreement with previous results and with a model of the columnar to cubic phase transition [31], based on the epitaxial relation between the {1 1 1} and {0 0 1} planes of the cubic and hexagonal lattices, respectively, found in lyotropic systems. This dependence upon temperature probably results from the increased bulkiness and folding of the aliphatic tails which induce the shift of the hydrophobic–hydrophilic balance as in the precursor column [32].

When considering the various mesophases identified over all for the different zwitterionic single chain amphiphiles, three additional features may be pointed out:

(a) The surface area S (45 ± 3 Å^2) available per chain at the interface remains close to twice the transverse area of a fully extended molten aliphatic chain, whatever the amphiphile and the type of liquid crystalline order. This constancy suggests that the aliphatic tails are arranged similarly in all three types of mesophase close to the interface. Nevertheless, despite the common contribution of thermal expansion, it is the type of structure which actually defines the opposing dependences of S upon temperature observed for the smectic A phase on the one hand and for the columnar and cubic phases on the other hand.

‡Strictly speaking, the number N_z of zwitterions should be given for a columnar unit of $1.0746S^{0.5}$, since it is supposed that the local arrangement is hexagonal, for which the average distance between neighbouring molecules is $(2/3^{0.5})^{0.5} S^{0.5}$.

(b) The zwitterionic domains never show spheroidal shape, in good agreement with theoretical calculations which disclaim spherical micelles for the segregated structures of *n*-hexyldimethylammonioalkylsulphonates ($p = 1, 3, 4$) [11].

(c) There is no specific evidence that different zwitterion conformations (extended vs. curled), as mentioned in §1, contribute in distinct ways to the mesophases observed in the amphiphiles studied (that is, by giving rise to two different mesophases depending on the conformation). On the other hand, the presence of a flexible tether may well play a role in the exact arrangement in the mesophases.

4. Conclusions

This study clearly shows that the long alkyl chain dimethylammonioalkoxydicyanoethenolates, *n-p*, are thermotropic amphiphiles. The driving force for the development of liquid crystal order at temperatures higher than the melting of the alkyl chains is the self-association of the highly dipolar zwitterionic groups through strong dipolar interactions [11] in an incompatible liquid paraffin matrix.

Mesophase thermal stability is highly favoured by longer paraffin tails, $n \geqslant 14$, and shorter tethers, p, in the zwitterionic moiety, as a result of an increase in the amphipatic properties of the thermotropes. Thus, the range of stability may extend over more than 100°C, as observed for 18-2 and 18-3. Furthermore, these thermotropes show a variety of liquid crystalline structures (smectic A, hexagonal columnar and inverted bicontinuous cubic phases), which depend on the n and p values, the columnar structure appearing alone in the amphiphiles with the lowest (and identical) ratio of alkyl tail to zwitterion length.

These amphiphiles may thus be considered as a new and interesting example among the still rather scarce series of homologous single chain thermotropes displaying a rich liquid crystalline polymorphism involving cubic phases [30, 31]. Their polymorphism is, in fact, similar to that determined for phasmidic and biforked mesogens [33] in that these also possess smectic, columnar and *Ia*3*d* cubic phases. In this connection, it may be noted that, in the latter, the bulkiness of the aliphatic portion is greater than that of the rigid moiety, whereas, in the zwitterionic amphiphiles, the opposite is true.

For a more comprehensive overall understanding of the thermotropic properties of this series of amphiphiles, it would be of interest to develop systematic chemical variations on the zwitterionic moiety based on the dicyanoethenolate structure: length and nature of the tail attachment (e.g. alkyl instead of alkoxy), rigidity and bulkiness of the tether, steric crowding at the ammonio site. Study of these molecular parameters should aid in defining the short range order (internal packing of the dipolar segments) and the cohesion (dipolar interactions) of the zwitterionic domains, and thus the type and the thermal stability of the long range liquid crystalline order typical of these thermotropes. The detailed arrangements of the zwitterions within the columns and rods of the columnar and cubic phases, as well as in the smectic A sublayers, also still need to be determined. In addition, the interplay between the cubic and smectic A phases in these materials, in particular involving the kinetics of the cubic phase development and possible contributing factors, bear further study.

Finally, as for our previous studies on segmented zwitterionomers and ionenes [4, 5], comparison between the zwitterionic and their homologous cationic amphiphiles (ammonium salts, see *b* in the scheme) should be quite fruitful. Dipolar (zwitterions) and coulombic (ion-pairs) interactions cannot be considered as completely identical, and they may lead to significant differences in the thermotropic properties of these two closely related series.

Mrs. S. Zehnacker and Mr. Pascal Vuillaume are gratefully acknowledged for their contributions to the DSC measurements. C.G.B. thanks NSERC (Canada) and FCAR (Québec) for financial support.

References

[1] Galin, J. C., 1996, in *Polymeric Materials Encyclopedia*, Vol. 9, edited by J. C. Salamone (Boca Raton: CRC Press), p. 7189.
[2] Middleton, W. J., and Engelhardt, V. A., 1958, *J. Am. chem. Soc.*, **80,** 2788.
[3] Galin, M., Chapoton, A., and Galin, J. C., 1993, *J. chem. Soc. Perkin Trans. 2*, 545.
[4] Grassl, B., Meurer, B., Scheer, M., and Galin, J. C., 1997, *Macromolecules*, **30,** 236.
[5] Grassl, B., Mathis, A., Raviso, M., and Galin, J. C., 1997, *Macromolecules*, **30,** 2075.
[6] Chrisment, J., Galin, M., and Galin, J. C., 1995, *New J. Chem.*, **19,** 303.
[7] Bazuin, C. G., Guillon, D., Skoulios, A., and Zana, R., 1986, *J. Physique*, **47,** 927.
[8] Tabrizian, M., Soldera, A., Couturier, M., and Bazuin, C. G., 1995, *Liq. Cryst.*, **18,** 475.
[9] Paleos, C. M., 1994, *Mol. Cryst. liq. Cryst.*, **243,** 159.
[10] Tschierske, C., 1996, *Prog. Polym. Sci.*, **21,** 775.
[11] Bredas, J. L., Chance, R. R., and Silbey, R., 1988, *Macromolecules*, **21,** 1633.
[12] Laughlin, R. G., 1978, in *Advances in Liquid Crystals*, Vol. 3, edited by G. H. Brown (New-York: Academic Press), pp. 42 and 99.
[13] Fontell, K., 1990, *Colloid Polym. Sci.*, **268,** 264.
[14] Michas, J., Paleos, C. M., Skoulios, A., and Weber, P., 1993, *Mol. Cryst. liq. Cryst.*, **237,** 175.
[15] Galin, M., and Marchal, E., 1996, *Polym. Adv. Techn.*, **7,** 50.
[16] Luzzati, V., Tardieu, A., Gulik-Krzywicki, T., and Reiss-Husson, F., 1968, *Nature*, **220,** 485.

[17] Gulik, A., Luzzati, V., De Rosa, M., and Gambacosta, A., 1985, *J. mol. Biol.*, **182,** 131.
[18] Ibn-Elhaj, M., Guillon, D., Skoulios A., Giroud-Godquin, A. M., and Maldivi, P., 1992, *Liq. Cryst.*, **11,** 731.
[19] Lide, D. R. (editor), 1993–1994, *Handbook of Chemistry and Physics*, 74 Edn (Boca Raton: CRC Press).
[20] Seurin, P., Guillon, D., and Skoulios, A., 1981, *Mol. Cryst. liq. Cryst.*, **65,** 85.
[21] De Vries, A., 1975, *J. Phys. Suppl.*, **Fasc. 3,** C-1
[22] De Vries, A., 1975, *Pramana, Suppl.*, **1,** 93.
[23] Gallot, B., Germanaud, L., Chevalier, Y., and Le Perchec, P., 1988, *J. coll. interf. Sci.*, **121,** 514.
[24] Bates, F. S., 1991, *Science*, **251,** 898.
[25] Dunkel, R., Hahn, M., Borisch, K., Neumann, B., Ruettinger, H.-H., and Tschierske, C., 1998, *Liq. Cryst.*, **24,** 211.
[26] Guillon, D., and Skoulios, A., 1977, *Mol. Cryst. liq. Cryst.*, **38,** 31.
[27] B. Heinrich (to be published).
[28] Tsukruk, V., Mischenko, N., Köberle, P., and Laschewsky, A., 1992, *Makrom. Chem.*, **193,** 1829.
[29] Diele, S., Brand, P., and Sackmann, H., 1972, *Mol. Cryst. liq. Cryst.*, **16,** 105.
[30] Shen, Y., Safinya, C. R., Fetters, L., Adam, M., Witten, T., and Hadjichristidis, N., 1991, *Phys. Rev. A*, **43,** 1886.
[31] Donnio, B., Heinrich, B., Gulik-Krzywicki, Th., Delacroix, H., Guillon, D., and Bruce, D. W., 1997, *Chem. Mater.*, **9,** 2951.
[32] Borisch, K., Diele, S., Goring, P., Kresse, H., and Tschierske, C., 1998, *J. mater. Chem.*, **8,** 529.
[33] Nguyen, H.-T., Destrade, C., and Malthête, J., 1997, *Adv. Mater.*, **9,** 375.